· Article · Advances in Polar Science
doi: 10.13679/j.advps.2018.4.00233 December 2018 Vol. 29 No. 4: 233-242

Identification of optical auroras caused by mantle precipitation with the aid of particle observations from DMSP satellites

HAN Desheng[1] & YANG Huigen[2]

[1] State Key Laboratory of Marine Geology, School of Ocean and Earth Science, Tongji University, Shanghai 20092, China;
[2] SOA Key Laboratory for Polar Science, Polar Research Institute of China, Shanghai 200136, China

Received 16 April 2018; accepted 19 September 2018

Abstract Particle observations of the Defense Meteorological Satellite Program (DMSP) show that discrete auroral structures commonly exist in the region of the plasma mantle, but the optical features of the aurora generated by particles from the plasma mantle (called 'mantle aurora' in this paper) have not been established. A comparison of 7-year optical auroral observations made at the Yellow River Station with conjugate particle observations obtained from the DMSP confirm that mantle auroras have common features and can be clearly identified from all-sky imager observations. The mantle auroras normally present as sporadic and weak auroral structures split poleward of the dayside auroral oval. They are observed in both the green and red lines with the intensity of the red line being greater than that of the green line. In this paper, we illustrate typical mantle auroras and provide statistics on 55 mantle aurora cases that are confirmed by particle observation by the DMSP. Statistical results show that the occurrence of the mantle aurora has no clear dependence on the IMF *By* and *Bz* conditions, but the motion of the mantle aurora strongly depends on the IMF *By*, which indicates that the generation of the mantle aurora is intimately related to the dayside magnetopause reconnection. With the fundamental criteria for distinguishing the mantle aurora presented in this paper, we will be able to independently identify the mantle auroras from ground optical observations. This will allow us to investigate the physical processes that occur in the plasma mantle by monitoring the evolution of the auroral forms.

Keywords mantle aurora, plasma mantle, dayside aurora, high-latitude aurora

Citation: Han D S, Yang H G. Identification of optical auroras caused by mantle precipitation with the aid of particle observations from DMSP satellites. Adv Polar Sci, 2018, 29(4): 233-242, doi:10.13679/j.advps.2018.4.00233

1 Introduction

The terminology 'mantle aurora' was first used by Sandford (1964) in the 1960s to describe a kind of 'subvisual' aurora equatorward of the auroral oval early whereas the terminology 'plasma mantle' was first used by Rosenbauer et al. (1975) in the 1970s to describe 'a persistent layer of tailward-flowing magnetosheath-like plasma inside of and adjacent to the magnetopause' poleward of the cusp. Meng and Akasofu (1983) later confirmed that the mantle aurora defined by Sandford (1964) is produced by the precipitation of energetic electrons that drift azimuthally from the plasma sheet in the midnight sector to the dayside magnetosphere during substorms. This means that the mantle aurora defined by Sandford (1964) has no relation with the commonly accepted conception of the plasma mantle and, in fact, is the diffuse aurora (Han et al., 2015; Sandholt et al., 1998a).

On the basis of an extensive survey of precipitating

* Corresponding author, E-mail: handesheng@tongji.edu.cn

particle data from the Defense Meteorological Satellite Program (DMSP), Newell et al. (1991a) illustrated how to distinguish different plasma regimes near the cusp region, which include the plasma mantle, low-latitude boundary layer (LLBL), cusp, boundary plasma sheet (BPS), and central plasma sheet (CPS). Newell et al. (1991b) also noted that discrete aurora features of particle precipitation, on both large and small scales, commonly exist in the mantle region and pointed out that a substantial portion of the dayside ionosphere lies on field lines that thread the plasma mantle. Previous studies established that discrete auroral forms are associated with field-aligned currents (e.g., Sandholt et al., 1998a; Kamide and Rostoker, 1977) and there are field-aligned currents in the plasma mantle (e.g., Iijima and Potemra, 1976). It is therefore expected that discrete auroras generated by precipitation particles from the plasma mantle, referred to as mantle auroras in this paper, will be observed in ground-based optical observations.

Optical auroras observed near the cusp region have been extensively studied. Sandholt et al. (1998a), for example, classified them into seven categories and systematically investigated their dependence on the solar wind and interplanetary magnetic field (IMF). Yang et al. (2000) noted that discrete auroras observed in the cusp region often have a coronary shape. Han et al. (2017, 2015) defined a particular aurora form, called the throat aurora, which is north–south aligned and only observed at the equatorward edge of the auroral oval. However, it remains unclear if auroras generated by precipitations from the plasma mantle can be distinguished from auroras generated by precipitations from other regions; this paper aims to find criteria for identifying mantle auroras.

In this paper, according to coordinated ground and satellite observations obtained from 2003 to 2009, we present typical cases that show that auroras generated by electrons from the plasma mantle have some common properties and can be distinguished in ground all-sky imager (ASI) observations. We also present a statistical study and discuss how to understand the observational properties of mantle auroras.

2 Data and method

The Chinese Yellow River Station (YRS), at Ny-Ålesund, Svalbard (having geographic coordinates of 78.92°N, 11.93°E, a magnetic latitude of 76.24°N, and a magnetic local time (MLT) of approximately +3.0 h universal time (UT)), is one of the few stations that can make longtime optical auroral observations at the cusp latitude on the dayside during the boreal winter on the Earth. Since November 2003, an optical observation system comprising three identical ASIs equipped with narrowband filters, centered at 427.8, 557.5, and 630.0 nm, has been installed at the YRS. Each imager of the system was equipped with a charge-coupled device camera with resolution of 512×512 pixels. Routine observations have been made with a temporal resolution of 10 s, which comprises exposure and readout times of 7 and 3 s, respectively (Hu et al., 2009).

The DMSP satellites are in nearly circular Sun-synchronous orbits at an altitude of about 835 km. Particle data from SSJ/4 instruments, which measure electrons and ions from 32 eV to 30 keV, were mainly used in this study. We extensively surveyed more than 2000 cases of DMSP F13, F15, F16, and F17 passing through the field of view (FOV) of the ASIs from October 2003 to January 2010. Plentiful simultaneous particle and optical observations of auroras provide an unprecedented opportunity to investigate new properties of dayside auroras. The IMF data are 1-minute OMNI data for which the time has been shifted to the nose of the bow shock and are taken from CDAweb (http://cdaweb.gsfc.nasa.gov/).

In this study, we first select all the data periods in which satellites passed through the FOV of the ASIs and then plot the aurora image, footprint of the satellite on the aurora image, solar wind conditions, and simultaneous DMSP particle spectrograms in the same figure. Finally, we visually examine all the plots to check the correspondence between the particle and optical observations of auroras and to confirm the source region of the auroras. The criteria for identification of the plasma mantle from DMSP observations are taken from Newell et al. (1991b). The identification is based especially on the associated soft ion spectra, which have a temperature range from a few tens of electron volts to about 200 eV. With the aid of the DMSP particle observations, we present typical cases of mantle auroras that were observed under different IMF conditions as follows.

3 Observation

3.1 Mantle aurora observed under an IMF of $By < 0$ and $Bz < 0$

Figure 1 shows the case of DMSP F16 passing through the FOV of the ASIs on 23 December 2003. The two left columns present the auroral images observed in green (557.7 nm) and red (630.0 nm) lines. From top to bottom, images observed at 1029:31 UT, 1029:51 UT, 1030:21 UT, and 1030:51 UT are respectively marked ‘a’, ‘b’, ‘c’, and ‘d’. The trace of the satellite in the FOV of the ASIs is shown by a yellow curve while the footprint of the satellite is indicated by a red circle in each panel. ‘M.N.’ and ‘M.S.’ respectively show the magnetic north (poleward) and south (equatorward) in the aurora image. East (dusk) and west (dawn) are labeled on the uppermost image of the red line and all images are oriented in the same direction. The right panels, from top to bottom, show the IMF *Bz* (black line) and *By* (red line) components, total energy flux ($eV \cdot cm^{-2} \cdot s^{-1}$ sr) of electrons (black dots) and ions (red dots), average energy (eV) of electrons (black dots) and ions (red dots), and spectrogram of

the differential energy flux of electrons and ions (Note that the ion energy scale is inverted). In the uppermost panel, we show the IMF *By* and *Bz* for a longer time period and the two dashed vertical lines indicate the time interval corresponding to the DMSP data plot. The four downward arrows mark the four moments ‘a’, ‘b’, ‘c’, and ‘d’. The magnetospheric regions identified using the method proposed by Newell et al. (1991b) are labeled under the downward arrows.

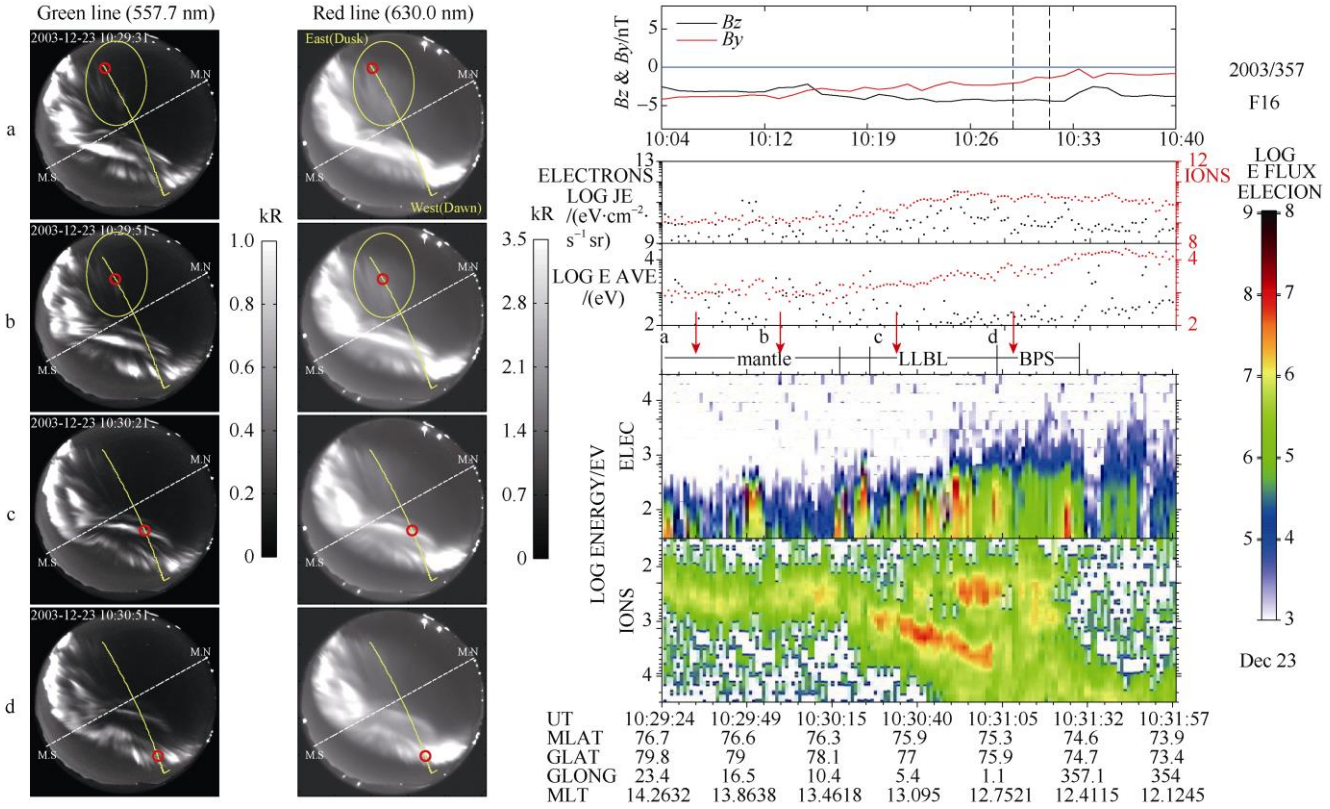

Figure 1 Case of DMSP F16 passing through the FOV of the ASIs on 23 December 2003 under southward IMF *Bz* at local noon.

According to the criteria for judging the plasma mantle given by Newell et al. (1991b), the spectrogram of Figure 1a has typical plasma mantle properties from 1029:24 UT to 1030:21 UT. Satellite F16 was passing the plasma mantle from moment ‘a’ to moment ‘c’. At moments ‘a’ and ‘b’, the ASIs observed a long auroral arc at the equatorward edge of the FOV and a dim, isolated auroral structure poleward of the long arc (marked by the yellow eclipse) in both green and red lines. The intensity in the red line is obviously greater than that in the green line for the dim auroral structure. Because the dim auroral structure was under the footprint of the satellite when the satellite observed the mantle property, we can reasonably refer to the dim auroral structure as a mantle aurora.

At moment ‘c’, the satellite was over a small auroral arc, which had just split from the long auroral arc and moved in the northeast direction. The spectrogram at moment ‘c’ also shows the mantle property, and we thus regard the small auroral arc observed under the footprint of the satellite at moment ‘c’ as the mantle aurora also. Considering the solar wind remained southward during this period, we suppose that this small aurora arc was a poleward moving aurora form (PMAF) resulting from magnetopause reconnection (Fasel, 1995). At moment ‘d’, the satellite was passing through the BPS and the ASIs observed a long aurora arc that was part of the main auroral oval.

To show the motion of the mantle aurora identified in Figure 1, we present the aurora images of the green line with 10-s intervals in Figure 2 and mark the mantle aurora with a black arrow. Figure 2 shows that the mantle aurora moves eastward (duskward) and both the IMF *By* and *Bz* are negative.

Figure 3 presents another pass of F16 through the FOV of the ASIs on 14 January 2004. During this pass, the ASIs observed two auroral structures in the FOV; i.e., a wide arc equatorward of the FOV and a narrow arc poleward of the wide arc. Satellite F16 is passing through the narrow arc at moment ‘c’ when the electron spectrogram presents the plasma mantle property, which confirms that the narrow arc is the mantle aurora. From images ‘a’ to ‘d’, we clearly see the mantle auroral arc split from the wide arc and move poleward. This is a PMAF and can be reasonably supposed to be generated by a magnetopause reconnection because the IMF *Bz* was southward in this case. Figure 3 presents a result consistent with Figure 1a; i.e., the PMAF that occurred most poleward of the auroral oval is the mantle aurora. Figure 3 also shows that the mantle auroral arc was observed in both green and red lines but the intensity was greater for the red line.

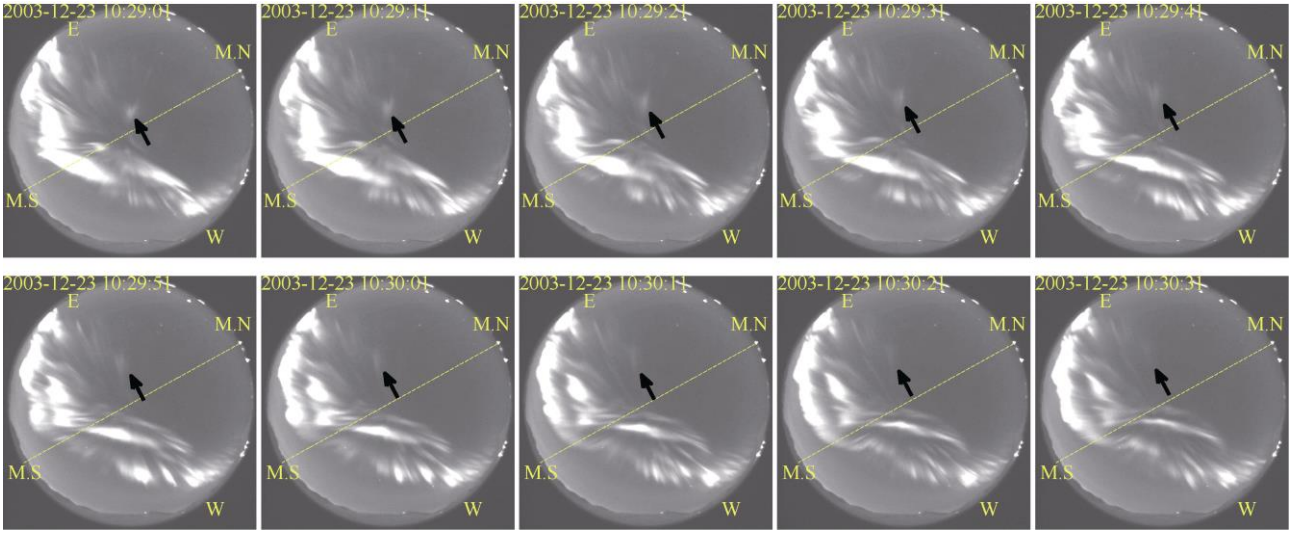

Figure 2 Aurora images in 10-s intervals for the case shown in Figure 1. Black arrows indicate the mantle aurora drifting duskward (eastward).

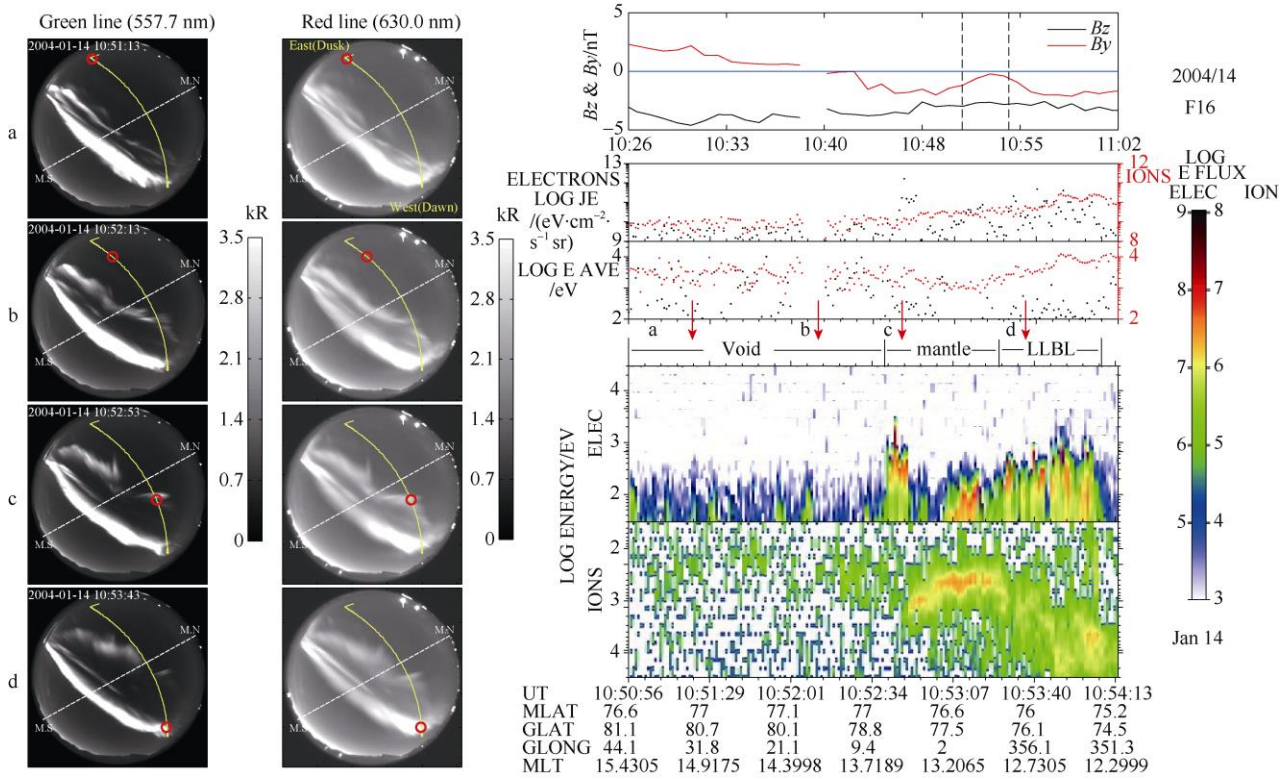

Figure 3 Case of DMSP F16 passing through the FOV of the ASIs on 14 January 2004 under southward IMF *Bz* near local noon.

Figure 4 presents aurora images as shown in Figure 3 with 10-s intervals. Figure 4 shows that the mantle aurora moves eastward (duskward) and poleward. Similar to the case shown in Figure 1, both the IMF *By* and *Bz* are negative for this event.

3.2 Mantle aurora observed under IMF *By* < 0 and *Bz* > 0

The above two cases were observed under the condition that IMF *Bz* < 0. Figure 5 presents the case observed on 27 November 2008 for the IMF *By* < 0 and *Bz* > 0. The spectrogram confirms that satellite F17 was in the plasma mantle at moment 'c'. A twisty auroral band was observed under the footprint of F17 at moment 'c'; this band split from a long auroral arc equatorward of the FOV and is identified as the mantle aurora. Figure 6 presents observations with 10-s intervals. We find that the twisty auroral band moves eastward (duskward) and poleward, as for the cases shown in Figures 1 and 3.

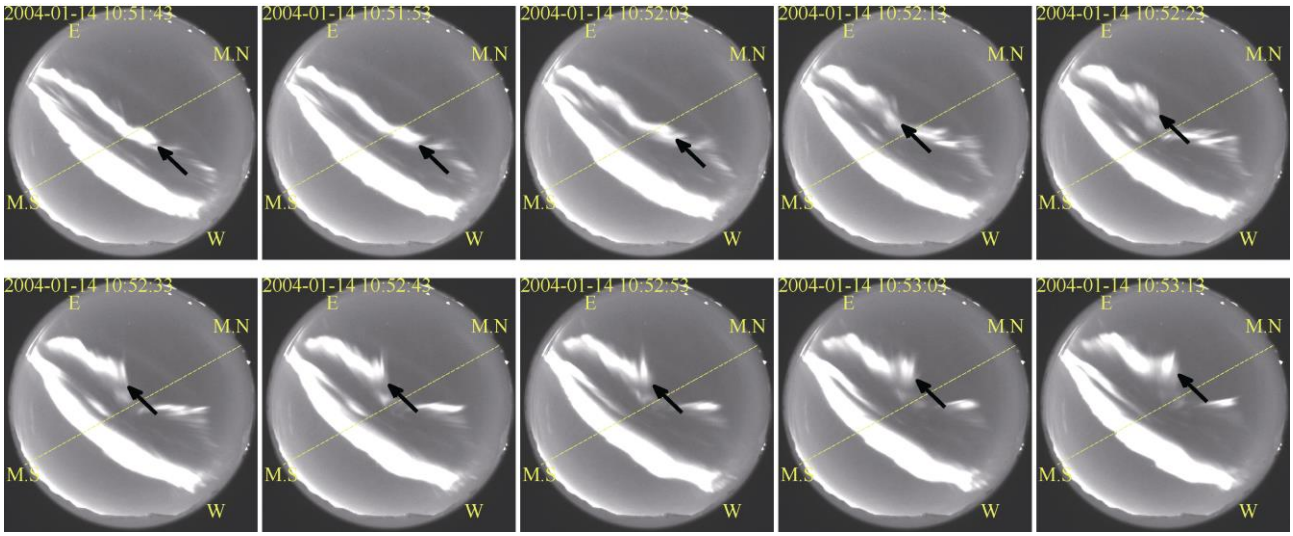

Figure 4 Aurora images in 10-s intervals for the case shown in Figure 3. Black arrows indicate the mantle aurora drifting duskward (eastward) and poleward.

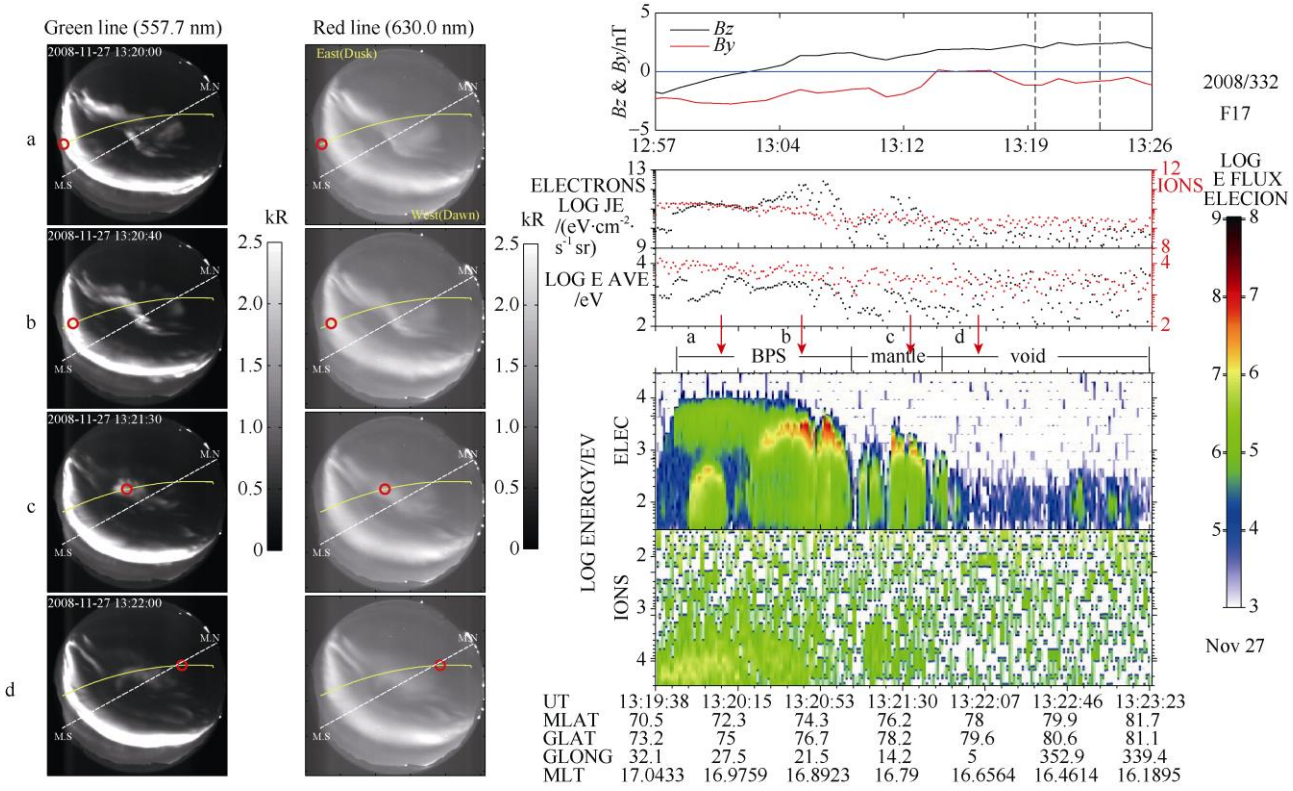

Figure 5 Case of DMSP F17 passing through the FOV of the ASIs on 27 November 2008 under northward IMF *Bz* in the postnoon.

3.3 Mantle aurora observed under IMF *By* > 0 and *Bz* < 0

All the above mantle auroras are observed under IMF *By* < 0 and show eastward (duskward) motion. Figure 7 presents an example case observed by the DMSP F13 satellite under the IMF *By* > 0 and *Bz* < 0 on 28 November 2006. The figure has the same format as Figure 1. In Figure 7, an aurora structure observed under the footprint of F13 at moments 'b' and 'c' is identified as the mantle aurora, which shows a dim and sporadic auroral structure located poleward of the main aurora oval and having greater intensity in the red line than in the green line. These features are similar to the cases identified above. The most important point is that the mantle aurora observed here clearly moves westward, as indicated by the yellow arrow

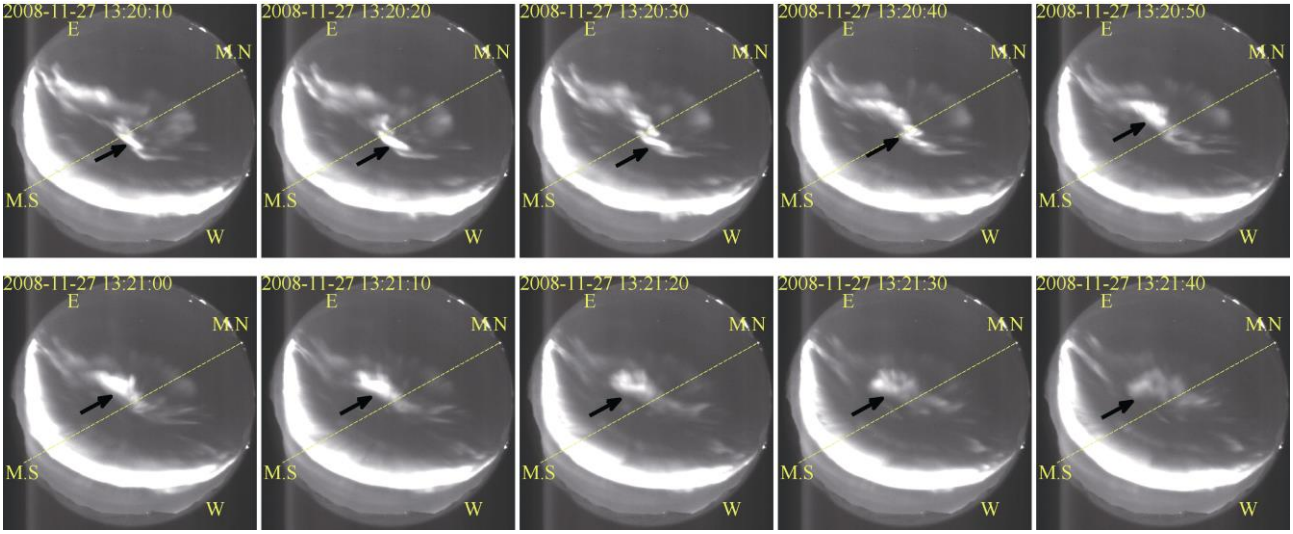

Figure 6 Aurora images in 10-s intervals for the case shown in Figure 5. Black arrows indicate the mantle aurora drifting duskward (eastward).

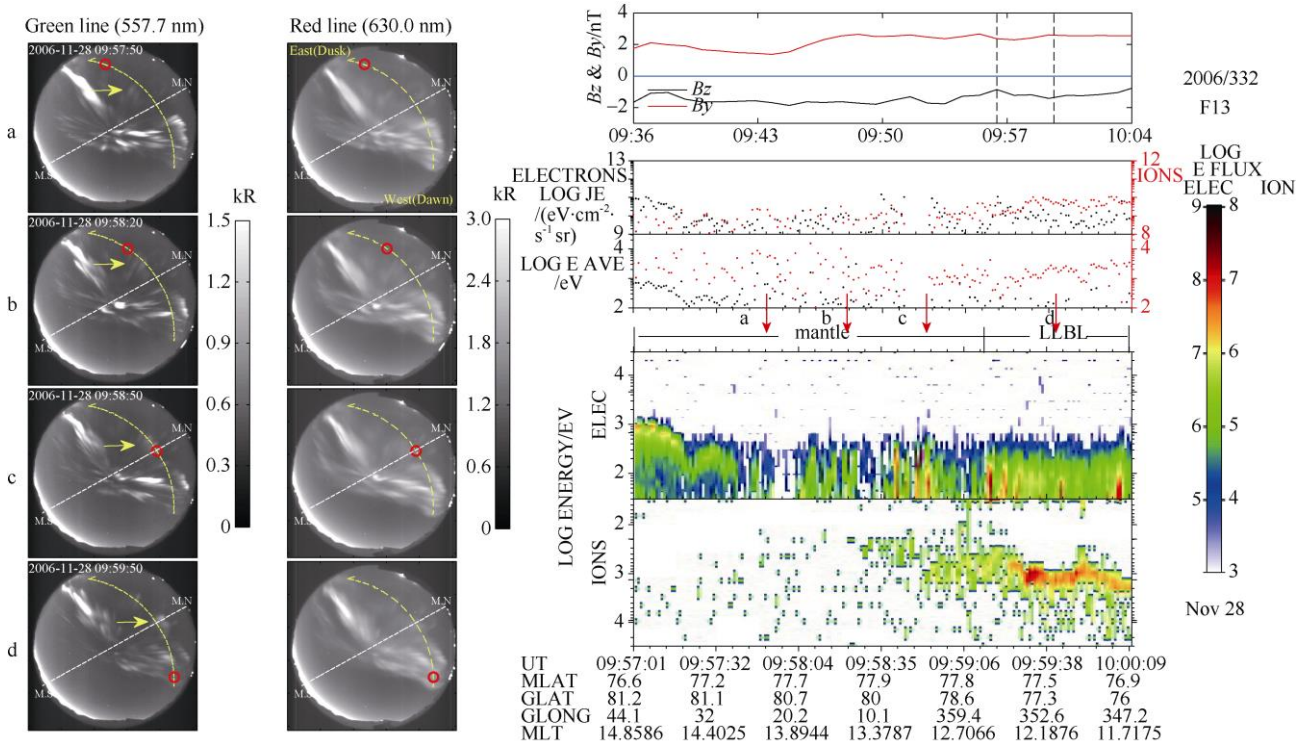

Figure 7 Case of DMSP F13 passing through the FOV of the ASIs on 28 November under southward IMF *Bz* and negative *By*.

on the images of the green line. This is opposite to what is observed under the IMF *By* < 0.

3.4 Mantle aurora observed under the IMF *By* > 0 and *Bz* > 0

To examine the motion of mantle aurora under different IMF conditions, we present a case observed under IMF *By* > 0 and *Bz* > 0 on 23 December 2006 in Figure 8. In this case, satellite F13 was continually located in the plasma mantle from moment 'a' to moment 'd' and the aurora structures observed under the satellite footprint are identified as the mantle aurora. These structures have common features as identified above; i.e., they are located poleward of the main oval, they are sporadic, and they have greater intensity in the red line. Additionally, we note that the mantel aurora structure, as indicated by the yellow arrow, moves westward (dawnward).

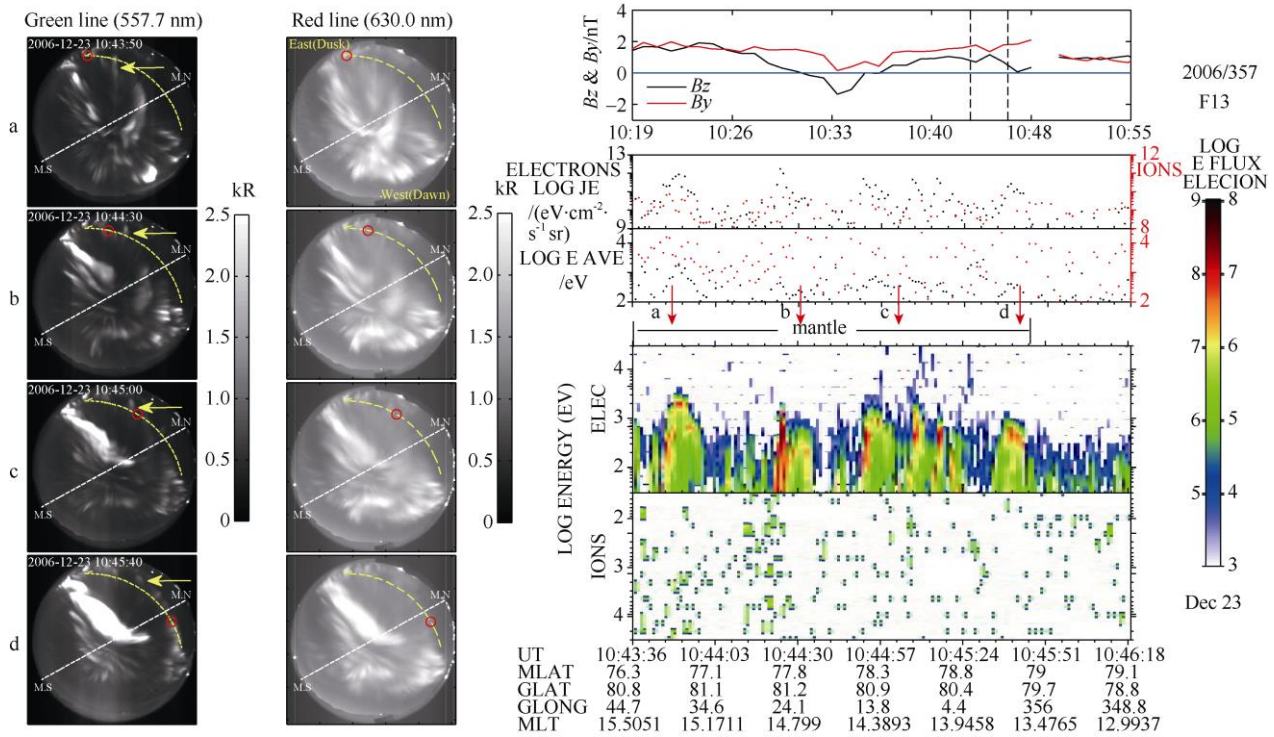

Figure 8 Case of DMSP F13 passing through the FOV of the ASIs on 23 December 2006 under northward IMF *Bz* and positive *By*.

3.5 Statistical study on the mantle aurora

The cases shown above indicate that the motion of the mantle aurora has a tendency to depend on the IMF *By*. To confirm this, we present statistical results in Figure 9. In our statistical analysis, we first selected all the mantle auroral cases (55 in total) that are identified by simultaneous optical and particle observations in the 7-year data and then made a movie for each case to examine the motion by visual inspection. Although the mantle auroras often move poleward, we here focus on examining their motion in the east–west direction. Each arrow in Figure 9 represents a mantle aurora case. The arrow directions on the left and right respectively indicate the motion of the mantle aurora toward the east (dusk) and west (dawn). Figure 9 presents the motion of the mantle aurora versus the MLT and IMF clock angle θ, where θ = arctan (*By*/*Bz*) and is estimated by taking the average for the case interval. Figure 9 shows that the motion of the mantle aurora strongly depends on the polarity of the IMF *By*; i.e., the mantle auroras predominantly move eastward (duskward) and westward (dawnward) for the IMF *By* < 0 and IMF *By* > 0, respectively.

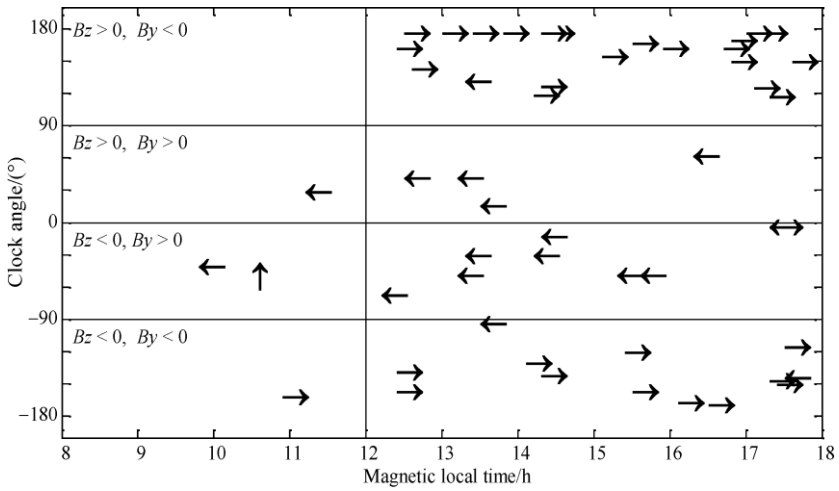

Figure 9 Statistical results of the east–west motion of the mantle aurora depending on the IMF clock angle, showing the almost unexceptional dependence on the IMF *By*.

4 Discussion

In this paper, we define the optical auroras generated by precipitations from the plasma mantle as the mantle aurora and show that the mantle auroras can be discriminated from ASI observations.

We found that the mantle auroras normally have sporadic auroral structures splitting poleward of the dayside auroral oval. The form of the mantle aurora can be a cluster of rays (as shown in Figure 1), a short arc (as shown in Figure 3), or a twisty aurora band (as shown in Figure 5). The main orientation of the mantle aurora is in the east–west direction and the intensity of the mantle aurora is normally not as strong as that of the auroras generated in the BPS/LLBL; i.e., of the main aurora oval. The mantel aurora can be observed in both the green and red lines and the intensity of the red line is normally greater than that of the green line. In our data set, the mantle auroras were mainly observed from ~0900 to ~1800 MLT and they can be observed under both northward and southward IMF conditions. Statistical results show that the mantle aurora moves eastward and westward under IMF $By < 0$ and IMF $By > 0$, respectively.

4.1 Mantle auroras and PMAFs

The dayside auroral forms and their dependence on the IMF and solar wind conditions have been extensively studied via ground optical observations made at Svalbard (Sandholt et al., 2004, 1998a, 1998b, 1998c, 1996a, 1996b, 1993, 1986). Sandholt et al. (1998a) classified the dayside auroral forms into seven types, among which the type-1 aurora observed under the southward IMF condition has a close relation to the mantle aurora identified in this paper. The type-1 aurora is observed at lower latitude (i.e., generally below 75° magnetic latitude (MLAT)) associated with a sequence of PMAFs (Sandholt et al., 1998a) that are characterized by a series of auroral brightening instances followed by poleward motion. The PMAFs are regarded as ionospheric signatures of a flux transfer event (Sandholt and Farrugia, 2007a, 2007b; Sandholt et al., 2004; Fasel, 1995). In this study, we found that the PMAFs observed at the poleward edge of the aurora oval, including those just splitting from the main auroral oval (as shown in Figure 1a at moment 'c'), correspond to mantle precipitations. This is consistent with previous studies on PMAFs. Sandholt and Farrugia (2007b) revisited the relationships among PMAFs, plasma convection, and field-aligned currents in the pre-noon and postnoon sectors under positive and negative IMF *By* conditions and found that the major brightening of PMAF, called auroral form 'A' by the authors, is followed by forms 'B' and 'C' located at higher latitudes. Form 'C' is weak compared with forms located at lower latitudes and is confirmed to be caused by mantle precipitation. We note that the optical property of the form 'C' aurora shown in Figure 3 of Sandholt and Farrugia (2007b) is consistent with that of mantle auroras presented in this paper. Sandholt and Farrugia suggested that form 'C' (i.e., the mantle aurora) is associated with an upward field-aligned current on the polar-cap side of the plasma convection channel and with pulsed reconnection. Rosenbauer et al. (1975) have long proposed that mantle particles can come from the cusp through reconnection. That is to say, when a pulsed reconnection occurs at the magnetopause under the southward IMF condition, the particles in the newly opened flux tube have a mantle property and the resulting auroras are observed as PMAFs.

We here stress that the PMAFs occurring at the poleward edge of the aurora oval are generated by mantle precipitation. We note that there are PMAFs equatorward of the aurora oval (Moen et al., 1996; Sandholt and Newell, 1992), where precipitation regimes (including the BPS or LLBL) are found (Sandholt and Newell, 1992). Sandholt et al. (1993) found the PMAF fades at the latitude of mantle precipitation. Moen et al. (1996) indicated that the PMAF originating at the LLBL moves poleward into regions of the cusp and mantle precipitation owing to the evolution of newly opened field lines.

It has generally been accepted that PMAFs are the ground signature of flux transfer events that are associated with magnetopause reconnections. The initial motion of the newly opened field lines depends on the balance of the magnetic tension force and forces exerted by magnetosheath flow (Cowley et al., 1983). For a negative (positive) IMF *By* component, magnetic merging is favored to occur along the dawn (dusk) flank of the magnetopause in the Northern Hemisphere and the newly opened magnetic field lines are dragged by the magnetic tension force duskward (dawnward). Therefore, the mantle auroras observed under the southward IMF could simply be understood as the footprints of the newly opened field lines, which drift duskward (dawnward) under negative (positive) IMF *By*. Under a northward IMF condition, the mantle auroras may correspond to newly reconnected field lines between the solar wind and lobe. In addition, although the studied events in Figure 9 have a bias toward the afternoon sector, they also show clear occurrence dependence on the IMF *By* component. It is clear, for example, that there are more afternoon events for $By < 0$ (35 events) than for $By > 0$ (13 events). The ratio is ~2.7, which is significant. The result is consistent with previous results (e.g., Sandholt et al., 2004) and can be explained by dayside magnetopause reconnection.

4.2 Mantle auroras and type-2 auroras

In the seven categories of dayside auroras defined by Sandholt et al. (1998a), type-2 auroras are observed under northward IMF conditions and possess the following properties. (1) They are observed at higher latitude (~78°–79° MLAT) during the period of positive IMF *Bz* in the clock angle range $\theta < 45°$ (Sandholt et al., 1998a, 1998b). (2) They appear as a rather stable, continuous

auroral band (Sandholt et al., 1996) or rayed auroral structure with moderate intensity (Sandholt et al., 1998a, 1998c). (3) They have IMF *By*-related east–west motions (Sandholt et al., 1998a). (4) They show equatorward motion in latitude (Sandholt et al., 1998c). The type-2 aurora is interpreted as an ionospheric signature of reconnection between the IMF and the terrestrial lobe field in the high-latitude magnetopause (Sandholt et al., 1998c), and it has been suggested to result from cusp/mantle precipitation (Sandholt et al., 1998a). Sandholt et al. (2002) mentioned that the type-2 aurora occurred in the plasma mantle and presents as a PMAF. These properties of type-2 auroras, including the occurrence location and motions, are consistent with those of the mantle aurora. Most importantly, the cited studies indicated that type-2 auroras are caused by particles from the plasma mantle, which conforms to the definition of mantle aurora given in this paper.

4.3 Mantle auroras and auroral forms observed by satellite

We found that mantle auroras are sporadic auroral structures that split immediately poleward of the main aurora oval. Several previous studies noted discrete auroras poleward of the main auroral oval. Murphree et al. (1990), for example, observed auroral forms poleward of the aurora oval using an ultraviolet (UV) imager on the Viking satellite under a northward IMF and suggested that merging on the front surface of the magnetotail was involved in these emissions. On the basis of a UV imager observation made by the IMAGE satellite, Frey et al. (2004, 2003) examined localized, high-latitude dayside auroras (HiLDAs) and found that HiLDAs were more frequent in the summer season when the IMF *Bz* and *By* are both positive. Frey et al. (2003) suggested that a HiLDA is the optical signature of electron precipitation in the upward leg of a current system that closes the downward leg of the current system into the cusp in the ionosphere. We here suppose that the auroral forms observed by the UV imager on the satellite reported by Frey et al. (2004, 2003) and Murphree et al. (1990) are generated in the mantle region, and they can thus be called mantle auroras. The mantle aurora, as shown in Figures 3 and 5, can extend several hundred kilometers in longitude and split from the main auroral region at around ~1.0 degrees in latitude. The satellite UV imager can certainly observe these auroral forms. In addition, Frey et al. (2003) showed that the energy and flux of the precipitation particles are low, which is similar to what we present here for the mantle aurora. Murphree et al. (1990) and Frey et al. (2004, 2003) focused on showing the dependence of such auroras on certain IMF conditions, but did not discuss the dynamic properties that we investigated in the present study.

5 Summary and comments

Auroras generated by precipitation from the plasma mantle have been previously reported in various ways but they have never been systematically treated. In the present study, using coordinated optical observations obtained at the YRS and particle observations from DMSP satellites, we first defined all the auroras generated by particles from the plasma mantle as ‘mantle auroras’ and then demonstrated that all mantle auroras have some common features and can be distinguished from ground observations.

This study is important in that it not only gives a classification of mantle auroras but also improves our understanding of auroras at the poleward edge of the aurora oval on the dayside. In previous studies, both particle observations (Newell et al. 2004, 1991a, 1991b) and UV imager observations (Frey, 2004, 2003; Murphree et al., 1990) have shown the existence of mantle auroras but have not shown the two-dimensional dynamic properties of the mantle aurora. The dependence of the east–west motion of the mantle auroras on the IMF *By* shown in Figure 5 is informative in clarifying the generation of mantle auroras.

We note that this study is predominantly based on a technique for identifying the plasma regimes that was proposed by Newell et al. (1991a, 1991b), which is often questionable, especially in terms of judging the plasma mantle. If we understand the plasma mantle as a regime related with processes of reconnection followed by field line draping, there will be auroral brightening followed by a PMAF. It is therefore better to make a judgement by combining particle precipitation observations made by DMSP satellites with two-dimensional continuous optical observations made by a ground-based all-sky camera, just as we do in this paper, which may allow a more reliable judgement, at least for the regime of the plasma mantle.

Acknowledgments This work was supported by the National Natural Science Foundation of China (NSFC) (Grants nos. 41831072, 41774174, 41431072, 41474146, and 41674169). The DMSP particle detectors were designed by Dave Hardy of AFRL, and data were obtained from JHU/APL. The ASI data were provided by the Polar Research Institute of China. We appreciate very much three anonymous reviewers for their helpful and constructive comments on the manuscript of this paper.

References

Cowley S W H, Southwood D J, Saunders M A. 1983. Interpretation of magnetic field perturbations in the Earth’s magnetopause boundary layers. Planet Space Sci, 31(11): 1237-1258.

Fasel G. 1995. Dayside poleward moving auroral forms: A statistical study. J Geophys Res, 100: 11891-11906.

Frey H U, Immel T J, Lu G, et al. 2003. Properties of localized, high latitude, dayside aurora. J Geophys Res, 108(A4): 8008, doi:10.1029/2002JA009332.

Frey H U, Østgaard N, Immel T J, et al. 2004. Seasonal dependence of localized, high-latitude dayside aurora (HiLDA). J Geophys Res, 109: A04303, doi:10.1029/2003JA010293.

Han D S, Chen X C, Liu J J, et al. 2015. An extensive survey of dayside

diffuse aurora based on optical observations at Yellow River Station. J Geophys Res-Space, 120(9): 7447-7465, doi:10.1002/2015ja021699.

Han D S, Hietala H, Chen X C, et al. 2017. Observational properties of dayside throat aurora and implications on the possible generation mechanisms. J Geophys Res-Space, 122(2): 1853-1870, doi:10.1002/2016ja023394.

Hu Z J, Yang H, Huang D, et al. 2009. Synoptic distribution of dayside aurora: Multiple-wavelength all-sky observation at Yellow River Station in Ny-Ålesund, Svalbard. J Atmos Sol-Terr Phy, 71(8): 794-804, doi: 10.1016/j.jastp.2009.02.010.

Iijima T, Potemra T A. 1976. Field-aligned currents in the dayside cusp observed by Triad. J Geophys Res, 81: 5971-5979.

Kamide Y, Rostoker G. 1977. The spatial relationship of field-aligned currents and auroral electrojets to the distributions of nightside auroras. J Geophys Res, 82: 5589-5608.

Meng C I, Akasofu S I. 1983. Electron precipitation equatorward of the auroral oval and the mantle aurora in the midday sector. Planet Space Sci, 31: 889-899.

Moen J, Evans D, Carlson H C, et al. 1996. Dayside moving auroral transients related to LLBL dynamics. Geophys Res Lett, 23(22): 3247-3250, doi:10.1029/96gl02766.

Murphree J S, Elphinstone R D, Hearn D, et al. 1990. Large-scale high-latitude dayside auroral emissions. J Geophys Res, 95: 2345-2354.

Newell P T, Ruohoniemi J M, Meng C I. 2004. Maps of precipitation by source region, binned by IMF, with inertial convection streamlines. J Geophys Res, 109(A10), doi:10.1029/2004ja010499.

Newell P T, Wing S, Meng C I, et al. 1991a. The auroral oval position, structure, and intensity of precipitation from 1984 onward: an automated on-line data base. J Geophys Res, 96: 5877-5882.

Newell P T, Burke W J, Meng C I, et al. 1991b. Identification and observations of the plasma mantle at low altitude. J Geophys Res, 96: 35-45.

Rosenbauer H H, Gnmwaldt M D, Montgomery G, et al. 1975. Heos 2 Plasma observations in the distant polar magnetosphere: The plasma mantle. J Geophys Res, 80: 2723-2737.

Sandholt P E, F Denig W, Farrugia C J, et al. 2002. Auroral structure at the cusp equatorward boundary: Relationship with the electron edge of low-latitude boundary layer precipitation. J Geophys Res, 107(A9): 1235, doi:10.1029/2001ja005081.

Sandholt P E, Farrugia C J. 2007a. Poleward moving auroral forms (PMAFs) revisited: responses of aurorae, plasma convection and Birkeland currents in the pre- and postnoon sectors under positive and negative IMF *By* conditions. Ann Geophys, 25: 1629-1652.

Sandholt P E, Farrugia C J. 2007b. Role of poleward moving auroral forms in the dawn-dusk auroral precipitation asymmetries induced by IMF *By*. J Geophys Res, 112, A04203, doi:10.1029/2006JA011952.

Sandholt P E, Farrugia C J, Denig W F. 2004. Dayside aurora and the role of IMF |*By*|/|*Bz*|: Detailed morphology and response to magnetopause reconnection. Ann Geophys, 22, 613.

Sandholt P E, Farrugia C J, Moen J, et al. 1998a. A classification of dayside auroral forms and activities as a function of interplanetary magnetic field orientation. J Geophys Res, 103: 23325-23346.

Sandholt P E, Farrugia C J, Moen J, et al. 1998b. Dayside auroral configurations: Responses to southward and northward rotations of the interplanetary magnetic field. J Geophys Res, 103, 20,279.

Sandholt P E, Farrugia C J, Cowley S W H. 1998c. Pulsating cusp aurora for northward interplanetary magnetic field. J Geophys Res, 103, 26: 507.

Sandholt P E, Farrugia C J, Stauning P, et al. 1996a. Cusp/cleft auroral forms and activities in relation to ionospheric convection: Responses to specific changes in solar wind and interplanetary magnetic field conditions. J Geophys Res, 101: 5003.

Sandholt P E, Farrugia C J, Oieroset M, et al. 1996b. Auroral signature of lobe reconnection. Geophys Res Lett, 23: 1725.

Sandholt P E, Moen J, Rudland A, et al. 1993. Auroral event sequences at the dayside polar cap boundary for positive and negative interplanetary magnetic field *By*. J Geophys Res, 98: 7737.

Sandholt P E, Newell P T. 1992. Ground and satellite observations of an auroral event at the cusp/cleft equatorward boundary. J Geophys Res, 97(A6): 8685-8691.

Sandholt P E, Deehr C S, Egeland A, et al. 1986. Signatures in the dayside aurora of plasma transfer from the magnetosheath. J Geophys Res, 91, 10: 063.

Sandford B P. 1964. Aurora and airglow intensity variations with time and magnetic activity at southern high latitudes. J Atomos Terr Phys, 26: 749-769.

Yang H, Sato N, Makita K, et al. 2000. Synoptic observations of auroras along the postnoon oval: a survey with all-sky TV observations at Zhongshan, Antarctica. J Atmos Sol-Terr Phy, 62(9): 787-797, doi:10.1016/S1364-6826(00)00054-7.